

Laughlin-liquid–Wigner-solid transition at high density in wide quantum wells

Rodney Price

Department of Physics, University of Maryland, College Park, Maryland 20742

Xuejun Zhu

Department of Physics and Astronomy, Rutgers University, Piscataway, New Jersey 08855

S. Das Sarma

Department of Physics, University of Maryland, College Park, Maryland 20742

P. M. Platzman

AT&T Bell Laboratories, Murray Hill, New Jersey 07974

(Received 4 October 1994)

Assuming that the phase transition between the Wigner solid and the Laughlin liquid is first order, we compare ground-state energies to find features of the phase diagram at fixed ν . Rather than use the Coulomb interaction, we calculate the effective interaction in a square quantum well, and fit the results to a model interaction with length parameter λ roughly proportional to the width of the well. We find a transition to the Wigner-solid phase at high density in very wide wells, driven by the softening of the interaction at short distances, as well as the more well-known transition to the Wigner solid at low density, driven by Landau-level mixing.

In the past few years, experiments with two-dimensional electron systems in a perpendicular magnetic field have shown a long-expected behavior as the strength of the field increases. At comparatively low fields, the now-familiar fractional quantum Hall effect appears, as the longitudinal resistivity ρ_{xx} falls exponentially to zero as the temperature $T \rightarrow 0$ at fractional filling factors ν . As the field increases, however, an insulating state appears, with $\rho_{xx} \rightarrow \infty$ when $T \rightarrow 0$.^{1–3} Optical experiments^{4,5} show a new spectral line developing at the same fields. This behavior is commonly thought to signal the presence of a Wigner solid, predicted many years ago, and pieces of an experimentally derived phase diagram between the Wigner solid and the fractional quantum Hall (FQHE) or Laughlin liquid can be sketched out.

There are several experimental parameters that affect the boundary between Wigner solid and FQHE liquid.^{6–9} The most important is the magnetic filling factor $\nu = 2\pi n\ell^2$, where n is the electron density and the magnetic length $\ell = (\hbar c/eB)^{1/2}$. The FQHE appears only at certain fractional filling factors $\nu = p/q$, where p, q are integers and q is odd. The Wigner solid exhibits no such detailed dependence on ν , but becomes gradually more favorable as the particles are localized with decreasing ν . Also important is the electron density n , parametrized by the ion-disk radius $r_s = (\pi n)^{-1/2}$. (Here we use atomic units, where length is measured in units of the Bohr radius $a_B = \hbar^2/me^2$ and energy in units of e^2/a_B .) As the Landau-level separation is $\hbar\omega_c = 2/\nu r_s^2$, the energy cost of localizing the particles by Landau-level mixing falls rapidly with increasing r_s at fixed ν , until at some critical r_s the Wigner solid becomes more favorable than the FQHE liquid and the system freezes.

Finally, the experiments are all done in real systems, which must be considered quasi-two-dimensional, with some

finite thickness L characterizing the width of the electron layer. On average a pair of electrons is separated in the z direction by $\lambda < L$, so their effective interaction at distances $r \ll \lambda$ in the xy plane becomes much softer than the Coulomb interaction, while at large distances $r \gg \lambda$, the interaction is essentially Coulombic. This preserves the long-range character of the interaction while weakening the short-range part. Because the formation of the Wigner solid is driven by the long-range part of the interaction, while the FQHE liquid derives its energy advantage from the short-range part, the quasi-two-dimensional character of a real experimental system might be expected to favor the solid somewhat. There have been several recent experiments and theoretical studies^{10,11} of finite thickness effects on the incompressible FQHE state and, in general, it is now well established that finite layer thickness tends to destroy incompressibility by reducing the short-range part of the Coulomb interaction. To the best of our knowledge, however, the enhancement of the Wigner solid phase by the finite thickness effect has not been examined theoretically.

In this paper, we study the quantitative effects of the three length scales ℓ , r_s , and particularly λ on the Laughlin-liquid–Wigner-solid phase diagram. We compare ground-state energies and excited states of variational wave functions for the Wigner solid and the FQHE liquid as both r_s and λ are allowed to vary. We find that at small λ , such as that found in GaAs heterojunctions, the zero-temperature phase transition from liquid to solid at large r_s does not vary much from the Coulomb case.⁸ At large λ we find that the FQHE liquid gives way to the Wigner solid at low density, as expected, but most unexpectedly, we find that the Wigner-solid phase dominates the FQHE liquid at high density as well. Only in an intermediate range of r_s does the liquid have lower energy than the solid when λ is large. The interplay

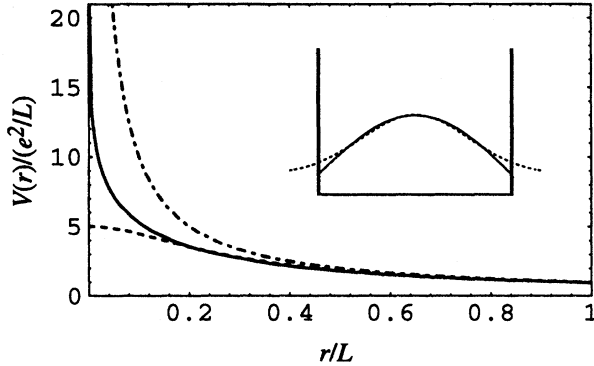


FIG. 1. The effective interaction (solid line), Coulomb interaction (dash-dotted line), and model interaction (dashed line) for a square well of width L . The model interaction parameter $\lambda = 0.2L$. The lowest subband cosine wave function and Gaussian fit are shown in the inset.

among the length scales ℓ , r_s , and λ can, in principle, therefore lead to a reentrant Wigner-solid transition at large λ as r_s is varied.

The electrons in a quantum well are confined to a small number of subbands, usually just one, and then can be thought of as extended rodlike charges in the z direction which are allowed to move only in the xy plane.¹² This approximation has been used in the past to study the weakening and eventual collapse of the FQHE state in a wide quantum well.¹¹ The interaction between these model charges is given by

$$V_{\text{eff}} = \int dz_1 \int dz_2 \frac{|\zeta(z_1)|^2 |\zeta(z_2)|^2}{[r^2 + (z_1 - z_2)^2]^{1/2}}. \quad (1)$$

Here $\zeta(z)$ is the envelope wave function describing quantization in the z direction and r is the separation between electrons in the xy plane.

The confining potential in the z direction enters into this equation only through the envelope wave function $\zeta(z)$. This wave function should be obtained in a self-consistent procedure which takes into account the interaction of the electrons in the xy plane. At low electron density, in quantum wells where the subband splitting is large, $\zeta(z)$ is simply the z component of the single-particle wave function. When electron density becomes higher, or the well is made wider bringing the subbands closer together, $\zeta(z)$ will be modified.

In a square well, however, λ and r_s are (roughly speaking) independent parameters, as the width of the well L is to lowest order independent of the density of the electrons in the xy plane. It is only when subband mixing begins to become important that the electron density begins to affect the envelope wave functions $\zeta(z)$. We expect that when only the lowest subband is occupied the single-particle wave functions will be adequate for $\zeta(z)$. The usual cosine solution for an infinite well is shown in the inset to Fig. 1, as well as a Gaussian wave function

$$\zeta_{\text{sq}}(z) = \frac{1}{(\pi\gamma^2)^{1/4}} e^{-z^2/2\gamma^2}, \quad (2)$$

fitted to the cosine solution. Here $\gamma = 0.277L$ gives the Gaussian wave function shown in Fig. 1. The effective potential for the two wave functions is almost identical. The Gaussian wave function gives

$$V_{\text{eff}}^{\text{sq}}(r) = \frac{1}{\sqrt{2\pi}\gamma} e^{r^2/4\gamma^2} K_0\left(\frac{r^2}{4\gamma^2}\right), \quad (3)$$

where K_0 is a modified Bessel function. We would like to use the simpler model interaction of Zhang and Das Sarma,¹³

$$V_0(r) = \frac{1}{\sqrt{r^2 + \lambda^2}}, \quad (4)$$

so we choose the parameter λ to fit $V_{\text{eff}}^{\text{sq}}(r)$ best when r is large. A least-squares fit, shown in Fig. 1, yields $\lambda/L = 0.2$.

Because λ/L is small for the square well, we need a wide well if we are to investigate a system with reasonably large λ . For example, a well with $\lambda = 1$ in an electron system in GaAs is approximately 500 Å wide. In these wide wells, subband mixing can become important, and the envelope wave functions will tend to spread out toward the edges of the well as the electrons reduce their potential energy. We have used the self-consistent approach taken in Ref. 10 to estimate the density distribution $n(z)$, and we find that λ/L will vary anywhere from 0.15 to 0.30 in the presence of subband mixing.¹⁴ If we choose the lowest subband value $\lambda = 0.2L$ for the square well, $V_0(r)$ is nearly identical to $V_{\text{eff}}^{\text{sq}}(r)$ for $r \geq 0.2L$, and differs significantly from $V_{\text{eff}}^{\text{sq}}(r)$ only for $r \leq 0.1L$. The pair correlation function for both liquid and solid is small below about $r = r_s$, so we believe $V_0(r)$ to be a good description of $V_{\text{eff}}^{\text{sq}}(r)$ for $\lambda \leq 2$.

In extremely wide quantum wells, $n(z)$ will be modified further as it peaks near the well edges. The well then begins to resemble a highly coupled double-layer system. Electrons in the well may lower their potential energy by localizing near the edges of the well, at the cost of some kinetic energy. In this more complicated situation, the approximation (1) begins to break down. At high density, the interaction between electrons that are adjacent in the xy plane becomes small, as they become separated in the z direction. The interaction between electrons localized on the same side of the well becomes stronger, however, and the net effect is a small potential energy savings. We should note, however, that the magnetic field will tend to suppress subband mixing, as at $\nu = 1/3$ the filling in the lowest subband will be at most 1/3.

In this paper, we determine the zero-temperature phase boundary between Wigner solid and Laughlin liquid by comparing ground-state energies of variational wave functions for the liquid and the solid. Because we are simply comparing energies, we are assuming that the phase transition is first order, and we neglect the possible presence of any other states in the vicinity. At high electron density we regard the approximation (1) as a qualitative guide only, and do not attempt to predict a critical r_s and λ quantitatively for the low r_s transition.

A variational wave function for the liquid which interpolates in some sense between a wave function with the lowest possible kinetic energy, the Laughlin wave function, and a wave function with the lowest possible potential energy, in which the electrons are completely localized, might be ex-

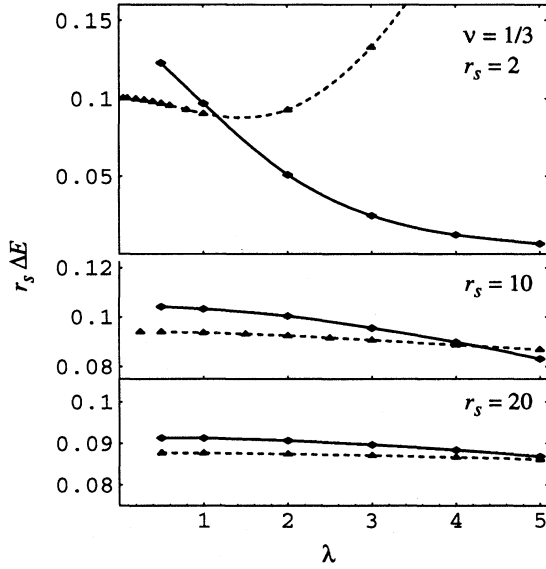


FIG. 2. The variational liquid energy (dashed line) and solid energy (solid line) shown after subtracting $\hbar\omega_c/2$ and the Madelung energy for various fixed values of r_s .

pected to be a good variational choice. To that end, we have chosen a variational wave function that consists of the Laughlin wave function ψ_m ($m=1/\nu$) multiplied by a Jastrow factor $\prod_{i<j} e^{-\alpha/\sqrt{r_{ij}}}$, where r_{ij} is the distance between the i th and j th particles and α is the variational parameter. When $\alpha=0$, we recover the Laughlin wave function, and when $\alpha \neq 0$, the wave function is no longer analytic and higher Landau levels are mixed in. The Jastrow factor introduces more correlations into the wave function, lowering the potential energy, while introducing a kinetic energy cost.

Details of the calculation are given in Ref. 8, so we will only review it briefly here. (Note that Ref. 8 uses units of energy $e^2/2a_B$, while this paper uses atomic units e^2/a_B .) We use the spherical geometry, in which our wave function becomes

$$\psi_m^\alpha = \prod_{i<j} (u_i v_j - u_j v_i)^m \exp\left(\frac{-\alpha}{|u_i v_j - u_j v_i|^{1/2}}\right), \quad (5)$$

where $u_i \equiv e^{-i\phi_i/2} \cos(\theta_i/2)$, $v_i \equiv e^{i\phi_i/2} \sin(\theta_i/2)$ are convenient spinor coordinates, and the distance between particles i and j is taken as the chord distance $r_{ij} = 2R|u_i v_j - u_j v_i|$. Evaluating the energy of this wave function by Monte Carlo and minimizing at a fixed r_s and λ gives the results shown by the dashed lines in Figs. 2 and 3.

In order to find the liquid-solid phase boundary we need a rather accurate evaluation of the solid. Lam and Girvin⁶ evaluated the energy of a correlated Wigner-solid wave function

$$\Psi = \exp\left(\frac{1}{4} \sum'_{i,j} \xi_i B_{ij} \xi_j\right) \prod_i \phi_{R_i}(z_i), \quad (6)$$

where $\xi_i = z_i - R_i$, $B_{ij} \equiv B(R_i - R_j)$, and

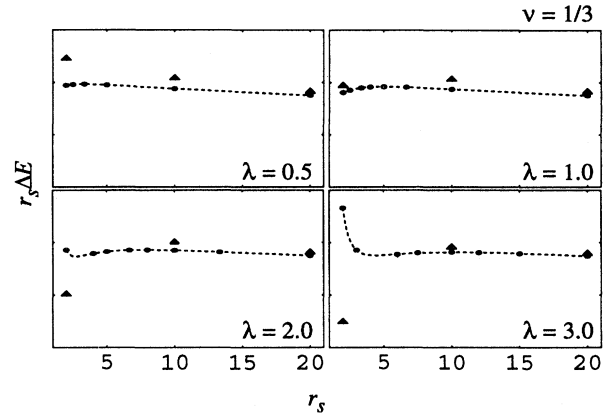


FIG. 3. The variational liquid energy (dashed line) and solid energy (triangles) shown after subtracting $\hbar\omega_c/2$ and the Madelung energy for various fixed values of λ .

$$\phi_{R_i}(z_i) = \exp\left\{-\frac{1}{4}[|z_i - R_i|^2 - (z_i^* R_i - z_i R_i^*)]\right\}. \quad (7)$$

Here $z_i = x_i + iy_i$ is the i th particle position and $R_i = X_i + iY_i$ is the i th lattice site. Ψ is the harmonic crystal wave function restricted to the lowest Landau level, and the variational parameters B_{ij} are calculated by using the values derived from the harmonic crystal. However, in order to make a reasonable comparison of solid and liquid wave functions, we need, as discussed above, a wave function which includes Landau-level mixing.

A study⁷ of the ground-state energy of the Wigner crystal including Landau-level mixing has recently been completed, using the Coulomb interaction. We have extended their work to use the modified potential (4). This calculation is similar to that of Lam and Girvin, except that two more variational parameters α and β are added to the wave function to put in more correlations at the expense of some Landau-level mixing. First, the Gaussians in the single-particle wave functions (7) were ‘‘squeezed’’ to move the electrons farther away from each other, by making the replacement

$$\exp\left(-\frac{1}{4}|z_i - R_i|^2\right) \rightarrow \exp(-\beta|z_i - R_i|^2). \quad (8)$$

Varying the parameter β away from $1/4$ introduces Landau-level mixing into the wave function because the single-particle wave functions $\phi_{R_i}^\beta(z_i)$ are no longer eigenstates of the single-particle Hamiltonian. An additional Jastrow factor is then introduced, and the final wave function, with two variational parameters α and β , is then

$$\Psi = \exp\left(\sum'_{i,j} \left[\frac{1}{4} \xi_i B_{ij} \xi_j - \frac{\alpha}{2} u(|z_i - z_j|)\right]\right) \prod_i \phi_{R_i}^\beta(z_i), \quad (9)$$

where

$$u(r) = \frac{1}{\sqrt{r}} (1 - e^{-\sqrt{r}F - r/2F}), \quad (10)$$

and F is a constant chosen to optimize the pseudopotential at small r . Zhu and Louie varied B_{ij} as well as β , but found that varying B_{ij} had very little effect on the energy, as Lam

and Girvin had suggested. The quantum Monte Carlo calculations were done with modified periodic boundary conditions,⁷ which require the addition of a phase factor to the single-particle wave functions (7). The results are shown as solid lines in Fig. 2 and the triangular data points in Fig. 3.

The $r_s=2$ curves in Fig. 2 are very nearly the lowest Landau-level energies, since $\hbar\omega_c$ is large at $r_s=2$. In fact, if each of the curves in Fig. 2 were plotted as a function of λ/r_s and there were no Landau-level mixing, they would lie on top of each other. Only the increased Landau-level mixing at $r_s=10$ and 20 reduces the energy there somewhat. The parameter λ/r_s can be thought of as the ratio of the average separation in the z direction λ and the average separation in the xy plane r_s (actually $\sim 2r_s$) of two nearby electrons. The lowest Landau-level energies cross at $\lambda=6$ at $r_s=10$ and $\lambda=12$ at $r_s=20$, but the variational energies here predict a freezing transition at $\lambda\approx 4$ at $r_s=10$ and possibly $\lambda\approx 6-7$ at $r_s=20$. These results illustrate the fact that Landau-level mixing does, in general, tend to favor the solid somewhat.

The variational wave functions use the fact that localizing the electrons by mixing in higher Landau levels will keep nearest-neighbor electrons farther apart, and since the Coulomb potential rises rapidly at small r the energy savings can be significant. As the interaction softens, however, the energy savings become small, and as a result the liquid and solid energies at $r_s=2$ are nearly identical to the lowest Landau-level energies. Ortiz, Ceperley, and Martin¹⁵ have recently used their fixed-phase quantum Monte Carlo method to improve the liquid energy shown here somewhat. The difference in energy is significant at $r_s=10$ and 20 , but at $r_s=2$ the change in energy for the Coulomb interaction is only ~ 0.006 , a shift on the order of 10%.

The rapid descent of the solid energy with λ leads to a freezing transition at about $\lambda=1.2$ at $r_s=2$, brought on by the softening of the short-range part of the interaction. Keeping the well width constant and lowering the density gives a smaller λ/r_s , and the system melts once again until the increased Landau-level mixing at high r_s causes the system to freeze again. Figure 3 shows the energies of solid and liquid

when λ is fixed and r_s is allowed to vary. At $\lambda=0.5$ we find no significant lowering of the solid energy at low r_s , but at $\lambda=1$ the solid energy at $r_s=2$ is nearly as low as the liquid energy, and at $\lambda=2$ and 3 the solid energy at $r_s=2$ is much lower than the liquid energy. In all cases the liquid becomes favorable at lower density until Landau-level mixing again causes the system to freeze. The transition at high density has been seen in the experiment of Suen, Santos, and Shayegan,¹⁰ where an insulating phase was observed in an 800-Å well at $\nu=1/3$, $r_s=1.7$, which became a well-defined FQHE state when the density was lowered to $r_s=2.2$.

We wish to emphasize again the qualitative nature of our calculation. The approximations leading to the model interaction V_0 begin to break down at high density and wide well width, where the system begins to take on a three-dimensional (3D) character as the coupling between subbands (neglected in our model) starts becoming important. In addition, as the interaction softens, the influence of impurities on the system is strengthened, and disorder plays a more prominent role. With these caveats in mind, however, we have shown that a softening of the interaction occurs at high density which may lead to a reentrant freezing transition in wide wells.

We can contrast the wide well (i.e., large λ) situation, which we have argued in this paper may be favorable to the solid phase both at large and smaller r_s , with the situation of a heterojunction with a metal gate which screens the interelectron Coulomb interaction, changing it to $V_{\text{eff}}(r\rightarrow\infty)\sim 1/r^3$ and $V_{\text{eff}}(r\rightarrow 0)\sim 1/r$. For the gated heterojunction case clearly the Laughlin liquid will be preferred because the effective interaction remains Coulombic for small r . Thus, careful experiments in which wide wells contrasted with those in gated heterojunctions would go a long way in establishing the liquid-solid phase boundary in strong-field 2D systems.

The authors wish to thank P. I. Tamborenea and Song He for helpful discussions, and P. I. Tamborenea for providing us with his data. This work was supported by the US-ARO, the US-ONR, and NSF.

¹R. L. Willett *et al.*, Phys. Rev. B **38**, 7881 (1988).

²H. W. Jiang *et al.*, Phys. Rev. Lett. **65**, 633 (1990).

³V. J. Goldman, M. Santos, M. Shayegan, and J. E. Cunningham, Phys. Rev. Lett. **65**, 2189 (1990).

⁴H. Buhmann *et al.*, Phys. Rev. Lett. **65**, 633 (1990).

⁵H. Buhmann *et al.*, Phys. Rev. Lett. **66**, 926 (1991).

⁶P. K. Lam and S. M. Girvin, Phys. Rev. B **30**, 473 (1984).

⁷X. Zhu and S. G. Louie, Phys. Rev. Lett. **70**, 335 (1993); (unpublished).

⁸R. Price, P. M. Platzman, and S. He, Phys. Rev. Lett. **70**, 339 (1993).

⁹P. M. Platzman and Rodney Price, Phys. Rev. Lett. **70**, 3487 (1993).

¹⁰Y. W. Suen, M. B. Santos, and M. Shayegan, Phys. Rev. Lett. **69**, 3551 (1992); M. Shayegan, J. Jo, Y. W. Suen, M. Santos, and V. J. Goldman, *ibid.* **65**, 2916 (1990).

¹¹S. He, F. C. Zhang, X. C. Xie, and S. Das Sarma, Phys. Rev. B **42**, 11 376 (1990); S. He, X. C. Xie, and S. Das Sarma, *ibid.* **47**, 4394 (1993).

¹²T. Ando, A. B. Fowler, and F. Stern, Rev. Mod. Phys. **54**, 437 (1982).

¹³F. C. Zhang and S. Das Sarma, Phys. Rev. B **33**, 2903 (1986).

¹⁴P. I. Tamborenea (private communication).

¹⁵G. Ortiz, D. M. Ceperley, and R. M. Martin, Phys. Rev. Lett. **71**, 2777 (1993).